

Pressure-induced transformations in glasses

V. G. Karpov and M. Grimsditch

Materials Science Division, Argonne National Laboratory, Argonne, Illinois 60439

(Received 26 March 1993; revised manuscript received 1 June 1993)

The double-well potential model, well known to describe many low-temperature properties of amorphous materials, has been extended to incorporate effects of high pressures. The resulting model not only explains the temperature and time dependences of pressure-induced phenomena but also provides possible explanations for thermal annealing effects as well as irradiation compaction. The results of Brillouin-light-scattering experiments designed to test various predictions of the model are presented: good agreement is obtained.

I. INTRODUCTION

There is now extensive experimental evidence that indicates that glasses undergo structural transformations when subjected to high pressures; in some cases these transformations are metastable after the pressure is removed. These transformations are usually evidenced by changes in the density,¹ sound velocity,² dielectric constant,³ and diffraction of x rays⁴ and neutrons.⁵ It is worth noting that, since the transformations exhibit no discontinuities and the properties of the material change smoothly as a function of pressure or time, these transformations are not connected with any phase transition in the strict thermodynamic sense as would be expected for a crystalline material.

The absence of qualitative changes and the smoothness of the observed property changes versus pressure enable us to infer that cooperative phenomena typical for "real" phase transitions, play only a minor role in these transformations. The integral of the changes in any macroscopic parameter of a glass can therefore be regarded as a result of successive accumulations of microscopic structural transformations in different local regions of a glass. The inherent randomness of glassy structures is a crucial consideration in this framework since it is fluctuations of structure parameters (bond lengths, valence, angles, etc.) that lead to the existence of local regions which react differently to pressure and time. It also accounts for the fact that, in turn, these transformations can be accumulated successively in time or under increasing pressure.

Here we present a model, based on a random double-well potential concept, which qualitatively describes pressure-induced transformations in glasses. The model, an extension of an earlier model used to explain low-temperature properties,^{6,7} is described in Sec. II. It yields predictions not only for pressure-induced effects but also for thermal treating and irradiation induced changes. In Sec. III we present experimental results on the temperature and time dependences of the relaxations in pressure-induced densified silica, and briefly review other existing relevant experiments. In Sec. III we compare the experimental results with the predictions of our model; we find that all observed effects can be understood in the

framework of the model proposed. In Sec. IV some concluding remarks are given.

II. THE GLASSY MODEL FOR STRUCTURAL TRANSFORMATIONS

Evidence for the existence of local bistable structures in glasses (irrespective of applied pressure) has been established by many authors in the course of investigations of a variety of low-temperature properties. In particular, it was shown that low-temperature specific heat, thermal conductivity, sound and electromagnetic wave absorption and propagation, and some other effects are universal in the sense that they are almost independent of the specific chemical composition of the glass. Because these properties are not typical of crystalline materials they are often called "anomalous," all of them were successfully interpreted in the framework of the double-well potential model proposed by Anderson, Halperin, and Varma⁶ and Phillips⁷ (see also the reviews⁸). This model suggests that in a glass a certain fraction of atoms retain some mobility (even at very low temperatures) moving in rather symmetric double-well potentials (see Fig. 1). The main double-well potential parameters; asymmetry (ϵ) and barrier height (V), are assumed to be uncorrelated random values uniformly distributed within corresponding intervals $0 < \epsilon < \epsilon_{\max}$ and $V_{\min} < V < V_{\max}$.

In the same spirit as the above model we consider a glass as a set of some structural units, each of which can exist in two different states corresponding to the minima

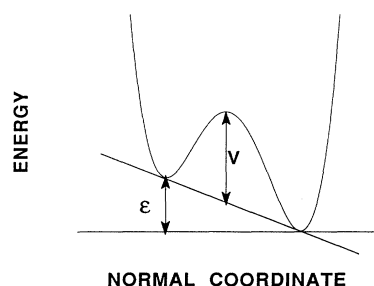


FIG. 1. Schematic diagram of the double-well potentials.

of the double-well potentials. We also assume that the parameters of the double-well potentials are pressure dependent. The normal state of each unit is, by definition, the one occupied at temperature $T=0$ and pressure $p=0$. At finite pressures shifts in the energy levels produce changes in the population of the different wells. These changes in turn affect the physical properties and, of particular relevance to this study, the density. At the temperatures of the experiments to be described, where tunneling effects can be neglected, the activation mechanism for interwell transitions leads to the relaxation time

$$\tau = \tau_0 \exp(V/T). \quad (1)$$

Strictly speaking, Eq. (1) should contain an additional multiplier $[\cosh(\epsilon/2T)]^{-1}$ which reflects the double-well potential asymmetry.⁹ Because $\epsilon \ll V$ (see Sec. III) we have omitted this factor for simplicity. The pressure (p) dependence of the double-well potential parameters are defined as follows:

$$\epsilon \rightarrow \epsilon + Dp \quad \text{and} \quad V \rightarrow V + Bp, \quad (2)$$

where D and B are deformation parameters and we consider only effects linear in p .

As was already mentioned above, it has been found that the disorder in a glass allows the parameters ϵ and V to be treated as random. The two new parameters D and B introduced here will also be treated as random, an assumption which must be confirmed *a posteriori*, but which is not unreasonable. One can imagine a variety of units with different atomic configurations but possessing the same values ϵ and V ; because these different configurations react differently to pressure, it means that they possess different deformation parameters. Note that the above arguments deal with the random nature of the parameters but not with their actual distribution. Information about the distribution of the parameters can be obtained from thermal expansion data which shows that the distribution of D values is almost symmetrical about the origin.¹⁰

Bearing in mind that the pressure-induced changes in macroscopic parameters are relatively small, one can suppose them to be proportional to the average change of the occupancy numbers of the double-well potentials states at pressure p (n_p) from those at zero pressure (n_0), viz. for a property v

$$\Delta v = A_v (\langle n_p \rangle - \langle n_0 \rangle), \quad (3)$$

where A_v is the change in the magnitude of the property v produced by a change in population of one double-well potential. In equilibrium at T and p we have

$$n_p = \{1 + \exp[(\epsilon + Dp)/T]\}^{-1}. \quad (4)$$

In general, however, n_p depends on time due to slow relaxation processes in the double-well potentials. Indeed, because of the range of barrier heights V , an exponentially wide spectrum of relaxation times is expected Eq. (1). Those structural units that have relaxation times that exceed the time of experiment do not contribute to observed change of macroscopic parameters. Note that ex-

perimental results on relaxation in glasses show that the spectrum of relaxation times spans over 12 orders of magnitude (roughly from 10^{-6} s up to 10^6 s), clearly overlapping usual experimental times.^{8,11}

The result of averaging in Eq. (3) depends on the particular shape of the probability distribution of random parameters. For the sake of simplicity we assume that the parameters are uncorrelated; for the same reason we assume their distribution to be uniform over given intervals:

$$\epsilon_1 < \epsilon < \epsilon_2;$$

$$V_1 < V < V_2, \quad D_1 < D < D_2, \quad \text{and} \quad B_1 < B < B_2. \quad (5)$$

Following the traditional double-well potential model^{6,7} we set $\epsilon_1=0$, furthermore we assume $\epsilon_2 \gg T$ reflecting the high degree of disorder in the system. Taking into account the fluctuations of the deformation parameter D mentioned above, we write $-D_1=D_2=D_0$, thereby neglecting a possible role of some small asymmetry of the distribution. Supposing that pressure induced changes of asymmetries ϵ and barrier heights V have the same origin, leads us to the simplifying (but nonessential) condition $-B_1=B_2=B_0$.

Because of the statistical independence of the parameters one can average firstly over parameters ϵ and D and secondly over the parameters V and B . The first step gives us thermodynamic equilibrium values (when setting $V=B=0$) that correspond to infinite time experiments. The second step averages over the relaxation time distribution where, according to Eqs. (1) and (2), the integration should be done over the interval

$$V_1 < V + pB < T \ln(t/\tau_0). \quad (6)$$

Here t is the time of the experiment. After these integrations Eq. (3) reduces to

$$\Delta v = A_v I(p, T) f(TL, p), \quad (7)$$

where

$$I = \langle \{1 + \exp[(\epsilon + Dp)/T]\}^{-1} - \{1 + \exp(\epsilon/T)\}^{-1} \rangle \quad (8)$$

is the change in the equilibrium average population of the double-well potentials and f is the fraction of double-well potentials which are kinetically able to change their states during the time t . We use the parameter L as an abbreviated notation for $L = \ln(t/\tau_0)$. The explicit form of f depends on the details of each experiment. We consider two typical cases: pressure-induced phenomena, and phenomena not involving pressure.

A. Pressure-induced phenomena

Within this section we again consider two examples: relaxation phenomena and annealing effects.

We consider first the general question concerning the change of $\langle n \rangle$ after a sudden change in pressure and temperature from their initial values p_i and T_i to the final values p_f and T_f . If we wait for infinite time the number of transformed states will be

$$\langle \Delta n(\infty) \rangle = I(p_f, T_f) - I(p_i, T_i). \quad (9)$$

Since for a particular double-well potential the decay rate is of the form

$$\{1 - \exp[-t/\tau(p_f, T_f)]\}, \quad (10)$$

where $\tau(p_f, T_f)$ is the relaxation [Eq. (1)] under the final conditions, and since by definition

$$f(p_f, T_f, t) = \langle 1 - \exp[-t/\tau(p_f, T_f)] \rangle, \quad (11)$$

we get

$$\Delta n(t) = [I(p_f, T_f) - I(p_i, T_i)]f(p_f, T_f, t). \quad (12)$$

1. Relaxation phenomena

The pressure is applied at zero time and we wish to determine the change Δv in a macroscopic parameter v after a time t at a fixed temperature T .

According to Eq. (12) the time dependence of any relaxation is given by $f(p_f, T_f, t)$. In accordance with Eq. (6) the fraction of transformed states is given by the shaded area in Fig. 2 bounded by the line $V = TL - pB$ (note that the position of this line is time dependent) and the other bounds of the parameters V and B distributions. As can be seen from Fig. 2 the area with vertical lines can be either a triangle or a trapezoid. Results for different cases are collected in Table I. The main conclusion is that f can depend either quadratically or linearly on $\ln(t)$, or is time independent, i.e., there is no relaxation.

2. Annealing procedures

The pressure, applied during a time t and at a temperature T , is removed and we wish to determine the relaxation after a time t' at a temperature T' (usually $T' > T$).

We consider the annealing procedure described above as a result of two successive steps. The first one is the change of pressure and temperature from $0, T_i$ to p_i, T_i , which according to Eq. (12) entails the change in the population

$$\langle \Delta n_1 \rangle = I(p_i, T_i)f(p_i, T_i, t)$$

[for simplicity we have taken $I(0, T) = 0$ which is equivalent to defining the $(0, T)$ state as the reference state]. The second step causes the change from p_i, T_i to $0, T_f$, providing the change in the population $\langle \Delta n_2 \rangle = -I(p_i, T_i)f(0, T_f, t')$. The total change is

$$\langle \Delta n \rangle = I(p_i, T_i)[f(p_i, T_i, t) - f(0, T_f, t')] \equiv I \Delta f. \quad (13)$$

Correspondingly, the measured hysteresis of a property v

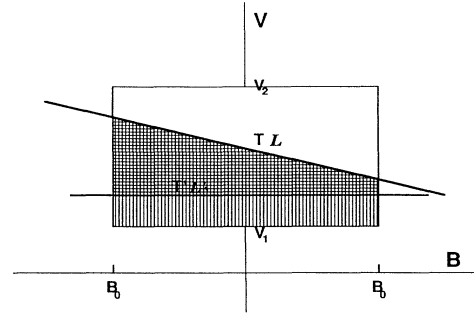


FIG. 2. Schematic diagram of the states in V - B parameter space which are "active" under various conditions of temperature T , pressure p , and time $t = \tau_0 \exp(L)$.

is $\Delta v_h = A_v I \Delta f$. Geometrically Δf is the area with horizontal lines in Fig. 2 between the lines

$$V = T' L' [= T' \ln(t'/t_0)]$$

and $V = TL - pB$, and the boundaries of the V and B distributions. For this case the results are summarized in Table II. Note that functions $f(p_i, T_i, t)$ and $f(p_f, T_f, t')$ in Eq. (13) generally correspond to different times t and t' as defined above, a feature which is reflected in Table II.

As can be seen from Table II in the general case $\Delta f \neq 0$ even if $T' = T$ and $t' = t$: this is an indication of a hysteresis phenomenon. The physical origin of the hysteresis is connected with the decrease of some potential barriers under the pressure. Due to this, the relaxation times of the corresponding double-well potentials decrease exponentially and allow a change to occur. The reverse changes require substantially longer times due to the increase in barrier heights after pressure removal.

Consider now the multiplier $I(p)$ given by Eq. (8) that determines in Eq. (7) the thermodynamic equilibrium changes. One of the integrals in Eq. (8) is

$$\langle [1 + \exp(\epsilon/T)]^{-1} \rangle = T \ln 2 / \epsilon_2. \quad (14)$$

Since the other integral in Eq. (8) cannot be calculated analytically we use regional approximations to obtain a qualitative picture

$$\begin{aligned} & \{1 + \exp[(\epsilon + Dp)/T]\}^{-1} \\ &= \begin{cases} 1 & \text{if } D < -\epsilon/p, \\ \exp[-(\epsilon + Dp)/T] & \text{if } D > -\epsilon/p. \end{cases} \end{aligned} \quad (15)$$

TABLE I. Relative concentration (f_1) of double-well potentials that change their states during the time $t = \tau_0 \exp(L)$ under the pressure p at temperature T .

No.	Conditions	f_1
1.	$V_2 > TL + pB_0 > V_1 > TL - pB_0$	$(TL + pB_0 - V_1)^2 / 4pB_0 \Delta V$
2	$V_2 > TL + pB_0 > V_1$	$(TL - V_1) / \Delta V$
3	$TL + pB_0 > V_2 > TL - pB_0 > V_1$	$1 - (pB_0 + V_2 - TL)^2 / 4pB_0 \Delta V$
4	$TL + pB_0 > V_2, TL - pB_0 < V_1$	$(TL + pB_0 - V_1)(TL + pB_0 - V_2) / 2p^2 B_0$
5	$TL + pB_0 < V_1$	0
6	$TL > V_2$	1

TABLE II. Relative concentration Δf of hysteretic double-well potentials produced by keeping a sample for a time $t = \tau_0 \exp(L')$ at temperature T' after removing the pressure p applied at temperature T during the time $t = \tau_0 \exp(L)$.

No.	Conditions	Δf
1	$T'L' < V_1$	0
2	$TL + pB_0 < V_2$, $TL - pB_0 > T'L'$	$(T'L' - TL)/\Delta V$
3	$TL + pB_0 > V_2$, $TL - pB_0 < V_1$	$\frac{(2pB_0 + 2TL - T'L' - V_2)(V_2 - T'L')}{4\Delta V p B_0}$
4	$TL + pB_0 > V_2$, $TL - pB_0 > T'L'$	$\frac{V_2 - T'L'}{\Delta V} - \frac{(B_0 p - V_2 - TL)(V_2 - TL + pB_0)}{4pB_0 \Delta V}$
5	$TL + pB_0 < V_2$, $TL - pB_0 < T'L'$	$\frac{(TL + pB_0 - T'L')(TL - T'L' + pB_0)}{4\Delta V p B_0}$
6	$T'L' > TL + pB_0$	f_1

Within the accuracy of not less than $\sim 10\%$ in all the range of parameters, it leads to the result

$$\begin{aligned} \langle \{1 + \exp[(\varepsilon + Dp)/T]\}^{-1} \rangle &= \left\{ \frac{D_0^2 p}{2} + TD_0 + \frac{T^2}{p} \left[1 - \exp \left[-\frac{D_0 p}{T} \right] \right] \right\} / (2\varepsilon_2 D) \quad \text{for } p < \frac{\varepsilon_2}{D_0}, \\ \langle \{1 + \exp[(\varepsilon + Dp)/T]\}^{-1} \rangle &= \left\{ -\frac{\varepsilon_2^2}{2p} + D_0 \varepsilon_2 + \frac{T^2}{p} \left[\frac{\varepsilon_2}{T} - \exp \left[\frac{D_0 p}{t} \right] \right] \right\} / (2\varepsilon_2 D) \quad \text{for } p > \frac{\varepsilon_2}{D_0}. \end{aligned} \quad (16)$$

In the limiting cases Eq. (8) has the form

$$\begin{aligned} I &\approx \frac{D_0^2 p^2}{12T\varepsilon_2} \quad \text{for } p \ll \frac{T}{D_0}, \\ I &\approx \frac{D_0 p}{4\varepsilon_2} - \frac{T}{\varepsilon_2} \left[\ln 2 - \frac{1}{2} \right] \quad \text{for } \frac{T}{D_0} \ll p \ll \frac{\varepsilon_2}{D_0}, \\ I &\approx 0.5 \quad \text{for } p \gg \frac{\varepsilon_2}{D_0}. \end{aligned} \quad (17)$$

B. Phenomena not involving pressure

In this subsection we consider some predictions of the model that are not connected with a pressure. One of them concerns heat treatments where our model predicts the possibility of a metastable expansion or contraction of a rapidly quenched glass. Suppose a glass is heated up to some temperature T' (which may also be less than T) kept at this temperature for a time t' and then rapidly quenched to the initial temperature T . At a time t after this procedure some properties may show a persistent change; in particular, if we consider the density change, $\Delta\rho(T)$, it is proportional to

$$\begin{aligned} \Delta\rho(T) &= A_p \langle [1 + \exp(\varepsilon/T')]^{-1} - [1 + \exp(\varepsilon/T)]^{-1} \rangle \\ &\quad \times [T' \ln(t'/\tau_0) - T \ln(t/\tau_0)] \\ &\approx A_p (T' - T)(T'L' - TL). \end{aligned} \quad (18)$$

Here the first term describes the change caused by the thermodynamic equilibrium occupation of expanded or contracted states of the double-well potentials when the temperature was high. The second term is connected with the kinetics and exhibits the difference between the relative concentrations of “active” double-well potentials at temperatures T' and T respectively. [Equation (18) assumes that the characteristic barrier heights TL and $T'L'$ are within the interval (V_1, V_2) ; otherwise the kinetic multiplier in Eq. (18) should be replaced by an appropriate expression from Table II taken at $p=0$.] A characteristic feature of the $\Delta\rho(T)$ given by Eq. (18) is the existence of an extremum (expansion or contraction) at a temperature

$$T' = T(L + L')/2L'. \quad (19)$$

The origin of this extremum is the competition between the kinetic and thermodynamic effects. Note that the thermally stimulated contraction and the existence of an extremum predicted by Eq. (17) does not include any masking effects due to thermal expansion and therefore provides an excellent possibility to verify our model.

Other predictions of the model are connected with the exposure of a glass to penetrating radiation or intense light. Suppose first that a glass is in equilibrium. Qualitatively the result of irradiation is expected to be the same as a heating to some effective temperature T_{eff} since both factors increase the transition rates in double-well potentials and provide a mechanism for populating the

higher-energy states. In this sense the situation appears to be qualitatively the same as in the case of thermal treatment described above. In particular, one can expect some contraction of a glass under irradiation. However, irradiation may also produce the opposite effect if the sample was in a nonequilibrium state induced by either pressure or quenching. In this case the effective radiation-related temperature (T_{eff}) can provide a sort of annealing effect leading to a corresponding expansion of the glass. Such an expansion will take place if the equilibrium state corresponding to the effective temperature T_{eff} is less contracted (or expanded) than the initial state before irradiation.

We summarize this section as follows: We have developed a model of extremely disordered systems that is reflected by the conditions $\epsilon_1=0$, $\epsilon_2 \gg T$, and suggestions about symmetric probability distributions of deformation parameters D and B . Although the model is essentially the same as the standard double-well potential model,^{6,7} its applicability to the regime of high pressures still needs experimental verification. The predictions of the model are as follows. (i) Nonelastic (microscopic) structural transformations take place in a glass under pressure which lead to corresponding changes of macroscopic parameters. These changes depend on pressure monotonically and saturate with increasing pressure. (ii) Over a very wide range of times, pressure-induced inelastic changes of structural parameters and their relaxation depend either linearly or quadratically on the logarithm of time multiplied by the temperature. (iii) Pressure-induced changes in a glass can reveal hysteretic phenomena on pressure removal. The magnitude of the hysteresis increases with pressure but reaches a saturation value. (iv) Property changes caused by thermal annealing and irradiation are also accounted for by the model.

We shall end this section with some remarks concerning alternative models of pressure-induced phenomena. The model described above presents the limiting case of an extremely disordered system. The exact opposite is the case of interacting identical units each of them described by an identical double-well potential where the role of disorder is assumed to be negligible. In this case the width of the transition due to thermal effects is of order of T/D . Since, to avoid considering a temperature driven transition, we must have $pD \gg T$, it follows that the main contraction must appear in a relatively narrow range of pressures. Such effects do indeed occur in some crystals but these steplike dependences differ qualitatively from the smooth dependences observed in glasses: One can also consider generalizations of the model in which the parameters of the double-well potentials are random but the characteristic fluctuations are not described by the assumptions we have made. If, for example, the low boundary of the asymmetry distribution is finite, i.e., $\epsilon_1 > 0$, then the pressure-induced effects will appear only if $T > \epsilon_1$ and/or $p > \epsilon_1/D_0$. Other conceivable modifications may entail changes in the symmetry of the distributions of the parameters B and D or postulate $\epsilon_2 < T$, etc. Such modifications lead to more complicated mathematical expressions but do not provide any new qualitative effects.

III. EXPERIMENTAL RESULTS AND COMPARISON WITH MODEL PREDICTIONS

Before dealing with any specific experiments we point out that the existence of pressure-induced hysteretic effects has been clearly established by a number of techniques. Most experiments have simply shown that a given property, e.g., density,¹ structure,^{5,12} etc., is different in a sample after it has been recovered from being subjected to high pressure. Raman scattering experiments¹³⁻¹⁵ have allowed this process to be followed as a function of pressure but yield only qualitative changes. One of the most clear indications of hysteresis loop type behavior was obtained from sound velocity measurements performed in a diamond anvil cell using Brillouin scattering.² These results are shown in Fig. 3. In comparing theory and experiment care must be taken to exclude nonhysteretic effects from the experimental data; for example, the velocity changes shown in Fig. 3 are largely elastic in nature so that only the *difference* between ascending and descending values can be compared with the present model.

All the experiments to be described below refer to α -SiO₂, and adequately reflect the fact that most experiments performed to date have been performed on this material. A few other examples of materials that do and do not show hysteretic effects will be discussed at the end of this section.

A. Temperature and irradiation

There have been many experimental investigations of the density changes of α -SiO₂ caused thermal treatment. Much of this information can be found in the review article by Primak.¹ In Fig. 4 we plot the density change of α -SiO₂ as a function of the quench temperature (Fig. 7 of Ref. 1). These results must be compared with the predictions of Eq. (18) with the caveats that neither the times involved in the experiments are specified, nor is the zero

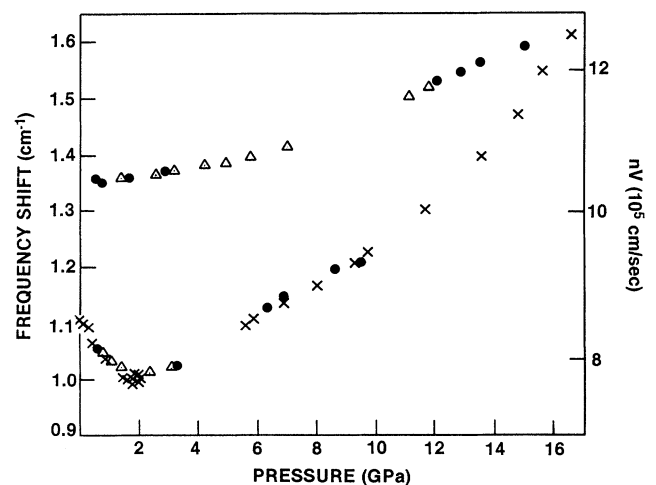


FIG. 3. Experimental sound velocities (Ref. 2) measured in α -SiO₂ as a function of increasing and decreasing pressure showing the existence of hysteretic effects.

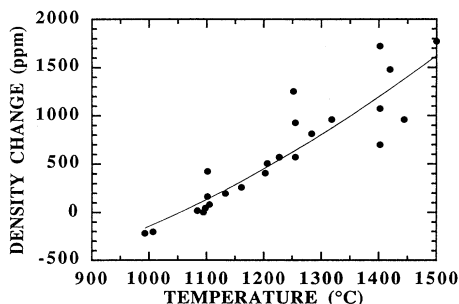


FIG. 4. Experimentally measured density changes (symbols) in α -SiO₂ as a function of quench temperature (Fig. 7 of Ref. 1). The full line is a fit according to Eq. (18) and is discussed in the text.

of the density changes well defined since the previous history of the samples is unknown. Qualitatively, the prediction of Eq. (18) regarding the existence of density changes caused by quenching is observed. Quantitatively the roughly quadratic behavior predicted by Eq. (18) (because in the experiments $T' \geq 1300$ K and $T = 300$ K) is not inconsistent with experiments, the spread and uncertainties in the data, however, are so large that all that can be concluded from such a comparison is that available data do not contradict the theoretical prediction.

A complete description of the effects of radiation is hampered by the same problems as those discussed in the previous paragraph. It is known, however (see review in Ref. 1), that particle irradiation of α -SiO₂ can either produce a compaction or reverse the compaction process depending on the preparation techniques and history of the initial sample. As briefly mentioned in Sec. II, these findings can be explained in the context of the present model.

The temperature dependence of the sound velocity in a sample which had been densified at room temperature up to a pressure of 18.2 GPa was presented in a Brillouin scattering investigation.¹⁶ The results, shown in Fig. 5, clearly show that the dependence is linear over a wide temperature interval (from 20 to 700 °C). In the frame-

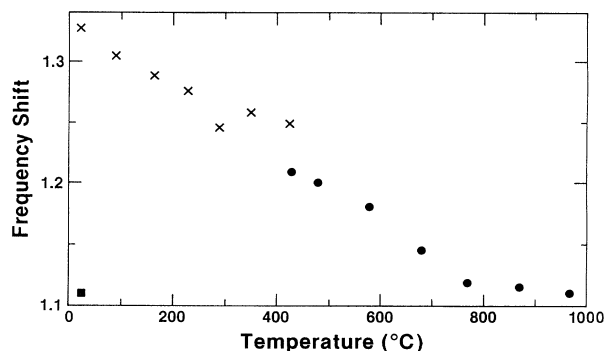


FIG. 5. Frequency shift (=sound velocity) vs temperature for a pressure densified α -SiO₂ sample (Ref. 16).

work of our model the linear temperature dependence of the relaxation means that $TL + pB_0 > V_2$ at $p = 18.2$ GPa; since otherwise the relaxation would also contain terms quadratic in T . Given the choice of possible behaviors predicted by theory, one again should be careful in assigning too much weight to the "agreement." The experiment can, however, be used to constrain the parameters of the model. From the characteristic temperature $T' \approx 1000$ K (above which there is no further relaxation) we can estimate the upper boundary of the barrier height distribution:

$$V_2 = T \ln(t/\tau_0) \approx 2.5 \text{ eV},$$

which is of the order of typical atomic barriers in solids.

B. Time

There is ample evidence in the literature that relaxation effects in glasses have a logarithmic time dependence. The time-dependent density changes in an α -SiO₂ sample heated to 993 °C (Ref. 1) clearly shows this logarithmic dependence over almost three decades. In Ref. 16 the time dependence of the room-temperature sound velocity in a sample which had been rapidly pressurized was investigated. It was observed that long times (~ 15 days) were required to reach equilibrium. Although no special attention was paid to accurately determine the form of this dependence, the results presented are consistent with a logarithmic time dependence as predicted by the model. Available data, however, do not address the issue of how this logarithmic dependence changes with temperature.

The following experiments were specifically designed to test, not only the logarithmic time dependence, but also the temperature dependence of its magnitude. Starting with small pieces of densified material¹⁷ we heated each piece to a known temperature and then measured the Brillouin frequency shift (i.e., sound velocity) as a function of time. (This experimental technique is described in Refs. 18 and 19.) The results of the experiments are shown in Fig. 6 and exhibit a linear dependence as a function of logarithm of time for the three temperatures measured. The model description is given by line 2 of Table II, viz.,

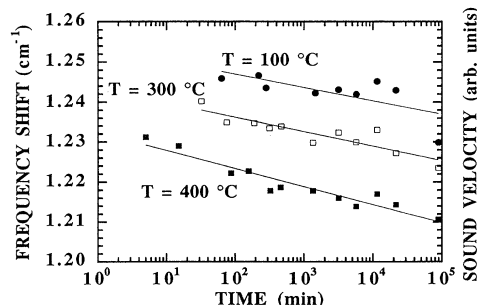


FIG. 6. Frequency shift (=sound velocity) vs time at various temperatures for a pressure densified α -SiO₂ sample. The full lines are fits according to Eq. (23).

$$\Delta\nu = \Delta\nu_0 - a(T \log_{10} t - T \log_{10} \tau_0), \quad (20)$$

where a is a proportionality constant. Fitting the experimental data to

$$\Delta\nu = M_0 + M_1 \log_{10} t, \quad (21)$$

we find that within the accuracy of the experiment, and as shown in Fig. 7, M_1 is proportional to T' in agreement with the prediction of Eq. (20). From the changes in M_1 and M_0 for the different temperatures, we also obtain the value of $\tau_0 = 10^{-(12 \pm 3)}$ s. This value is eminently reasonable since it corresponds to characteristic times of atomic vibrations in solids and therefore represents a reasonable estimate of the attempt frequency for barrier hopping.

C. Pressure

As stated at the beginning of this paper the main object of the present work was to explain phenomena related to pressure-induced densification, and the changes resulting to other physical properties. Before attempting to account for behavior such as that shown in Fig. 3, it must be noted that a sizeable portion of the pressure-induced changes in Fig. 3 are due to elastic effects, and as such, are not included in the model. Comparison with experiment can be simplified by comparing only experimental results in the starting and end material both at "zero" pressure. Such results (dots) are shown in Fig. 8 (Ref. 20); and correspond to the velocity change detected at zero pressure before and after pressurization to the maximum pressure P_{\max} . These results are then directly comparable with Eqs. (7) and (17) which, at least qualitatively, account for the observed effects.

A quantitative analysis of the results presented in Fig. 8 requires a knowledge of the parameters of the model appropriate for α -SiO₂. Some of the parameters are known: from the existence of anomalous behavior at very low temperatures we know that the parameters V_1 and ϵ_1 must be small [i.e., < 1 K (Ref. 8)]. Based on either the glass transition temperature, the melting temperature or the high-temperature annealing experiments discussed in

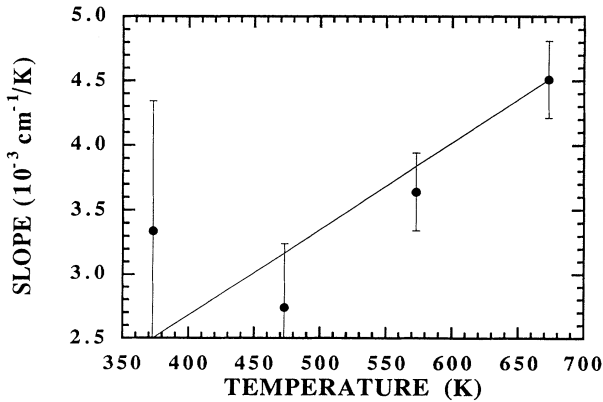


FIG. 7. Slope of the frequency vs time plots in Fig. 6 as a function of temperature. The full line is the expected scaling as T .

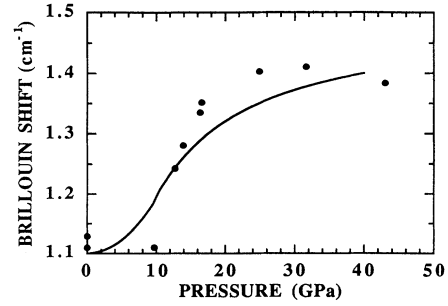


FIG. 8. Experimental [dots (Ref. 20)], hysteresis vs maximum pressure attained. The full line is obtained from the model as described in the text.

the previous section, we have $V_2 \approx 1.0-2.5 \text{ eV} \approx 2 \times 10^4 \text{ K}$. The value of the strain deformation parameter was estimated^{8,9} from ultrasonic experiments to be $\approx 1 \text{ eV}$, using the literature value for the bulk modulus yields $D_0 \approx 300 \text{ K/GPa}$. The only parameters for which there are no clear independent experimental data on which to base an estimate are B_0 and ϵ_2 . These parameters are critical for the model since they respectively determine the midpoints in $\Delta f(p)$ (Table II) and $I(p)$ [Eq. (17)]: we have chosen both parameters so that the midpoints of $f(p)$ and $I(p)$ are at 10 GPa. The values of the parameters used in the calculations below are summarized in Table III, those in brackets have been chosen to yield agreement with experiment. We note that for room-temperature experiments and reasonable experimental times ($t \approx 10^2-10^3 \text{ s}$) we have

$$T'L' \approx TL = T \ln(t/\tau_0) \approx 0.08 \text{ eV} (\approx V_2/3),$$

also, from the linear temperature relaxation discussed in the previous section, we have $TL + pB_0 > V_2$. Under these conditions, using the expressions 3 and 5 from Table II, we obtain the pressure dependence expected for Δf , which turns out to be similar to that of $I(p)$. Multiplying Δf by $I(p)$ [Eq. (13)] we obtain a function proportional to the pressure-induced hysteresis in any macroscopic parameter. After scaling the vertical scale to account for the unknown parameter A_v , we obtain the full line in Fig. 8 in reasonable agreement with the experimental values.

A few comments regarding our claim of "agreement" between theory and experiment for the results in Fig. 8 are in order. It should be clear that a number of parameters have been fitted to produce this agreement: the zero offset (which is unrelated to hysteresis), the overall scaling, and the B_0 and ϵ_2 parameters which determine the pressure scale of the effect. It could therefore be argued that the discrepancies between theory and experiment should really be the focus of the discussion. The most striking of these discrepancies is that the gradual onset of the effect predicted by theory is not observed experimentally. This can be seen in Eq. (17) which shows that the onset occurs at $\sim T/D_0$; better agreement could easily be produced by changing the parameter D_0 or even by arguing that the appropriate temperature is not that at which the experiments were performed but the fictive tempera-

TABLE III. Model parameters used in evaluating the full line in Fig. 8. Values in parentheses have been adjusted to produce agreement with experiment.

V_1	V_2	ϵ_1	ϵ_2	D_0	B_0
0 K	2.5×10^4 K	0 K	(3000) K	300 K/GPa	(800) K/GPa

ture from which the sample was quenched. It is also clear that by invoking a more complex distribution of parameters the theory could be made to fit the experiments "exactly." With the information currently available any such "improvement" in the model is not justified.

We conclude this section with a brief discussion of experimental results on materials other than α -SiO₂. The pressure dependence of Brillouin frequency shifts (sound velocity) have also been measured²¹ for α -GeO₂, α -B₂O₃, α -As₂S₃, and Lucite. Hysteresis effects were found in α -GeO₂ and α -B₂O₃ although not as pronounced as in α -SiO₂, but no hysteresis was found in either α -As₂S₃ or Lucite. These findings can be reconciled with our model by noting that α -As₂S₃ and Lucite are more labile systems compared with the other three glasses which show hysteresis; they also have lower coordination numbers and lower melting temperatures. These properties are likely to be indications of smaller characteristic barriers governing atomic motions. Consequently, it is not unreasonable that for these materials the condition $TL > V_2$ applies and, again based on Tables I and II, no hysteresis phenomena are predicted by the model.

IV. CONCLUSIONS

We have presented a model based on the concept of random double-well potentials which explains many as-

pects of the behavior of amorphous materials under high pressures and high temperatures. It accounts for the logarithmic time dependences observed in relaxation phenomena and also the temperature scaling of their magnitude. It qualitatively explains density changes caused by quenching and by irradiation. It also accounts for the hysteretic effects observed in samples recovered from high-pressure experiments.

A double-well potential model has been used to describe the strong perturbation effects ($\epsilon > 300$ K) caused by external pressure. Similar models (without the introduction of the deformation potentials) have, however, been used to describe high-energy perturbations, i.e., illumination^{22,23} or thermal treatments,²⁴ in α -Si:H. The results of the present work and those of Refs. 22–24 lead us to believe that the model of random double-well potentials has a much wider range of applicability than only the low-temperature properties of glassy materials.

ACKNOWLEDGMENTS

This work was supported by the U.S. Department of Energy, Basic Energy Science-Materials Sciences under Contract No. W-31-109-ENG-38.

¹William Primak, *The Compacted States of Vitreous Silica* (Gordon and Breach, New York, 1975).

²M. Grimsditch, Phys. Rev. Lett. **52**, 2379 (1984).

³B. A. Weinstein, R. Zallen, M. K. Slade, and A. de Lozanne, Phys. Rev. B **24**, 4652 (1981).

⁴Charles Meade, R. H. Hemley, and H. K. Mao, Phys. Rev. Lett. **69**, 1387 (1992).

⁵S. Sussman, K. J. Volin, D. L. Price, M. Grimsditch, J. P. Rino, R. K. Kalia, and P. Vashishta, Phys. Rev. B **43**, 1194 (1991).

⁶P. W. Anderson, B. I. Halperin, and C. M. Varma, Philos. Mag. **25**, 1 (1972).

⁷W. A. Phillips, J. Low Temp. Phys. **7**, 351 (1972).

⁸Yu. M. Galperin, V. G. Karpov, and V. I. Kozub, Adv. Phys. **38**, 669 (1989); S. Hunklinger and A. K. Raychaudhuri, in *Progress in Low Temperature Physics*, Vol. IX, edited by D. F. Brewer (Elsevier, Amsterdam, 1986), p. 155.

⁹A. R. Long, Adv. Phys. **31**, 553 (1982); W. A. Phillips, in "Phonons 89," edited by S. Hunklinger, W. Ludwig, and G. Weiss (World Scientific, Singapore, 1990), p. 367.

¹⁰D. A. Ackerman, A. C. Anderson, E. J. Cotts, J. N. Dobbs, W. M. MacDonald, and F. J. Walker, Phys. Rev. B **29**, 966 (1984); Yu. M. Galperin, V. L. Gurevich, and D. A. Parshin, *ibid.* **32**, 6873 (1985); V. G. Karpov, Pis'ma Zh. Eksp. Teor. Fiz. **55**, 59 (1992) [JETP Lett. **55**, 60 (1992)].

¹¹S. Sahling, A. Sahling, B. S. Negaev, and M. Colac, J. Low Temp. Phys. **65**, 289 (1986).

¹²P. McMillan, B. Piriou, and R. Couty, J. Chem. Phys. **81**, 4234 (1984).

¹³S. Mochizuki and N. Kawai, Solid State Commun. **11**, 763 (1972).

¹⁴R. J. Hemley, H. K. Mao, P. M. Bell, and B. O. Mysen, Phys. Rev. Lett. **57**, 747 (1986).

¹⁵G. E. Walrafen, Y. C. Chu, and M. S. Hokmabadi, J. Chem. Phys. **92**, 6987 (1990).

¹⁶M. Grimsditch, Phys. Rev. B **34**, 4372 (1986).

¹⁷The samples were small chips from a large sample pressurized to 16 GPa for a few hours: details are given in Ref. 5.

¹⁸J. R. Sandercock, in *Topics of Applied Physics*, Vol. 51 of *Light Scattering in Solids III*, edited by M. Cardona and G. Güntherodt (Springer, New York, 1982).

¹⁹W. Hayes and R. Loudon, *Scattering of Light by Crystals* (Wiley, New York, 1978).

²⁰A. Polian and M. Grimsditch, Phys. Rev. B **41**, 6086 (1990).

²¹M. Grimsditch, R. Bhadra, and Y. Meng, Phys. Rev. B **38**, 7836 (1988).

²²M. Stutzmann, J. B. Jackson, and C. C. Tsai, Phys. Rev. B **32**, 6873 (1985).

²³D. Redfield, J. Non-Cryst. Solids **97&98**, 783 (1987).

²⁴S. D. Albadergenova, N. A. Feoktistov, V. G. Karpov, K. V. Koughia, A. B. Pevtsov, and V. N. Solovijev, in *Transport, Correlation and Structural Defects*, edited by Helmut Fritzsche (World Scientific, Singapore, 1990), p. 129.